ChemComm

COMMUNICATION

View Article Online
View Journal | View Issue

Versatile functionalization of the NU-1000 platform by solvent-assisted ligand incorporation†

Cite this: *Chem. Commun.*, 2014, **50**, 1965

Received 8th November 2013,
Accepted 16th December 2013

DOI: 10.1039/c3cc48562e

www.rsc.org/chemcomm

Pravas Deria,‡[a] Wojciech Bury,‡[ab] Joseph T. Hupp*[a] and Omar K. Farha*[a]

Solvent-assisted ligand incorporation (SALI) was utilized to efficiently insert various carboxylate-derived functionalities into the Zr-based metal–organic framework NU-1000 as charge compensating moieties strongly bound to the Zr_6 nodes. SALI-derived functionalities are accessible for further chemical reactions such as click chemistry, imine condensation and pyridine quaternization.

Metal–organic frameworks (MOFs) represent a class of solid-state hybrid compounds consisting of multitopic organic struts and metal-based nodes which are interconnected by coordination bonds.[1] Crystalline and often highly porous, their chemical diversity and typically high surface areas[2] have been rendered attractive for a broad range of potential applications including gas storage and separation,[3] catalysis,[4] sensing,[5] and light harvesting.[6] Exploration of these applications can be facilitated by introducing new chemical entities into the MOF framework; however, *de novo* approaches to the incorporation of such entities are often problematic due to the formation of undesirable structures or side products during the MOF syntheses.[7] These issues, however, can be circumvented by turning to metal node functionalization (involving saturation of open coordinative metal sites),[8] and post-synthesis covalent modification[7,9] or replacement of the organic linkers using solvent-assisted linker exchange (SALE).[10]

MOFs derived from oxophilic Zr_6^{IV} nodes are promising candidates for employment in a wide range of functional applications due to their high thermal (up to 500 °C), chemical (pH 1–pH 11),[11] and mechanical stability.[11,12] Recently developed Zr-based mesoporous MOFs[13] are particularly attractive due to their large pores and channels that are expected to facilitate incorporation of new functionalities. For example, **NU-1000** (molecular formula $Zr_6(\mu_3\text{-OH})_8(\text{–OH})_8(\text{TBAPy})_2$; Fig. 1)[13a] contains $[Zr_6(\mu_3\text{-OH})_8(\text{–OH})_8]^{8+}$ nodes (or possibly $[Zr_6(\mu_3\text{-O})_8(\text{–OH}_2)_8]^{8+}$), where eight of the twelve octahedral edges are coordinated to TBAPy linkers (H_4TBAPy is the 1,3,6,8-tetrakis(*p*-benzoic-acid)pyrene). The eight terminal (*i.e.* non-bridging) –OH groups present opportunities for channel chemical modification – for example, reactive incorporation of metal ions *via* atomic layer deposition.[13a] Another node-centered route for channel chemical modification pathway is solvent-assisted ligand incorporation (SALI).[14] Functionalization *via* SALI entails an acid–base reaction between a carboxylic-acid-containing functional group (CFG) and a pair of terminal hydroxide ligands of the Zr_6 node, resulting in a daughter material **SALI-CFG**, where the charge compensating CFG ligands are strongly bound to the **NU-1000** node. This approach can be contrasted to conventional metal node functionalization wherein coordinatively unsaturated metal sites bind new ligands *via* dative bonds.[8a,b] Our previous work reported on the systematic functionalization of Zr_6 nodes with various fluoroalkanes.[14] Here we explore the chemical generality and group tolerance of the SALI approach using

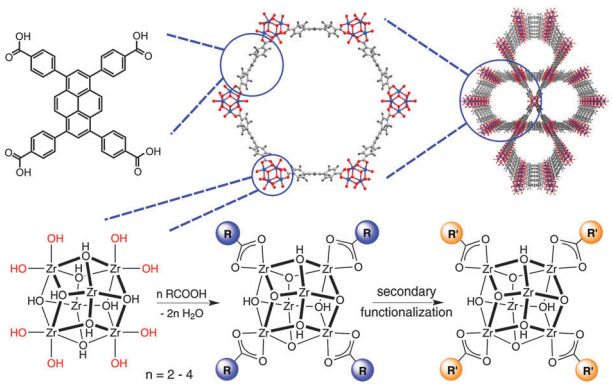

Fig. 1 Molecular representations of **NU-1000** (top); schematic representation of the SALI and secondary functionalization processes in the **NU-1000** platform (bottom).

[a] *Department of Chemistry, Northwestern University, 2145 Sheridan Road, Evanston, Illinois 60208, USA. E-mail: j-hupp@northwestern.edu, o-farha@northwestern.edu*

[b] *Department of Chemistry, Warsaw University of Technology, Noakowskiego 3, 00-664 Warsaw, Poland*

† Electronic supplementary information (ESI) available: Procedures, materials, and instrumentation; characterization (N_2 adsorption, BET, NMR spectra, and DRIFTS) of **SALI-n**. See DOI: 10.1039/c3cc48562e

‡ These authors contributed equally.

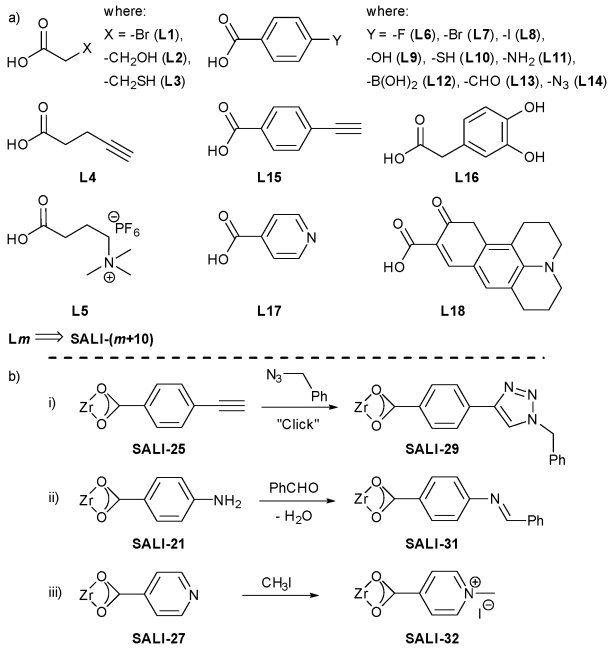

Scheme 1 (a) Carboxylic functional groups (CFGs) incorporated through SALI into **NU-1000**; (b) secondary functionalization reactions: (i) "click", (ii) imine condensation and (iii) methylation, involving SALI derivatives of **NU-1000**.

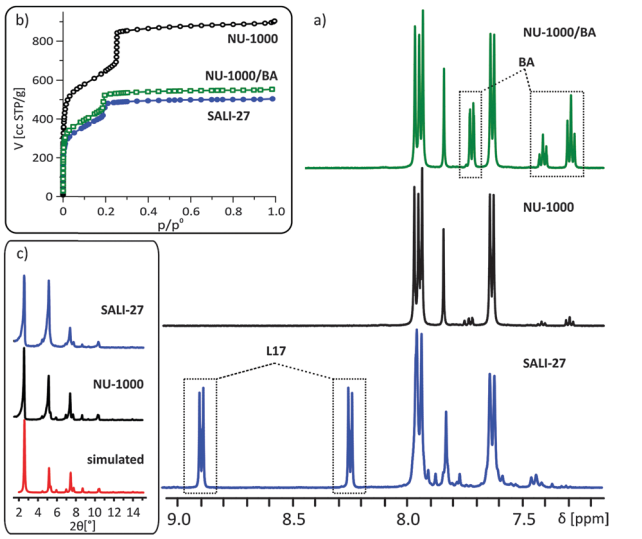

Fig. 2 (a) ^{1}H NMR spectra (b) N_2 adsorption isotherms, and (c) simulated and experimental PXRD patterns of **NU-1000** and the representative material **SALI-27**.

NU-1000 as a modification platform. Additionally we show that the large cavities and chemical robustness of the parent framework permit newly installed functional groups to be further chemically derivatized.

In our previous studies, we found that the as-synthesized form of **NU-1000**, termed **NU-1000/BA**, contains residual benzoate ligands at the node sites subsequently occupied by pairs of terminal hydroxides; see Fig. 1.[13a,14] Benzoate is present because benzoic acid was used as a modulator in the synthesis of **NU-1000**. Scheme 1a shows the range of carboxylates subsequently incorporated. For the majority of these, SALI proved possible only after removal of coordinated benzoate (by extended treatment of the as-synthesized material with aq. HCl in DMF at *ca.* 80 °C). Fig. 2a provides ^{1}H NMR spectroscopic evidence of benzoate removal; Fig. 2b shows that the removal is accompanied by a significant increase in the N_2-accessible pore volume (see below).

New carboxylate ligands were incorporated into activated microcrystalline samples of **NU-1000**[13a,14] by exposing the samples to solutions of 10 equiv. of CFG per Zr_6-node in polar solvents such as *N*,*N*-dimethylformamide (DMF), dimethyl sulfoxide (DMSO), acetonitrile (MeCN) or their mixtures at 60 °C for 24 h (see ESI† for a detailed description). For CFGs featuring lower pK_a values than that of benzoic acid (*e.g.*, compounds **L1** or **L6**) direct reaction of the ligand with **NU-1000/BA** was possible, with the substitution of benzoate by the CFG conjugate base occurring quantitatively. SALI reactions require a careful choice of a chemically compatible solvent – specifically, one that provides CFG solubility and that assists the acid–base chemistry involved in SALI reaction, including removal of the H_2O side product. It is worth noting that SALI was unsuccessful in solvent mixtures containing water. In most cases, DMF was successfully employed. For **L1**, **L4** and **L15**, however, SALI was unsuccessful in DMF, due to the formation and subsequent reaction of dimethylamine. This problem was overcome by using a 1 : 3 v : v mixture of DMSO and CH_3CN as solvent. For quantitative SALI of **L16**, pure MeCN proved suitable. Following SALI, the newly functionalized samples of **NU-1000** were soaked in fresh solvent to remove unreacted ligands. The samples were then thermally activated (*i.e.* solvent was removed) under reduced pressure.

The extent of CFG incorporation was estimated by ^{1}H NMR spectroscopy after dissolving each SALI-treated compound in a 10% D_2SO_4–DMSO-d_6 mixture (see Fig. 2a and ESI† Section S3). The corresponding signals of the incorporated CFG (Scheme 1) were integrated against that of the TBAPy ligand. Depending on the identity of the CFG, between 2 and 4 CFGs were incorporated per Zr_6 node[15] within **NU-1000** (Table S1, ESI†).

It is useful to note that complete functionalization entails incorporation of four carboxylate ligands per node, and results in an idealized-**UiO-66**-like node coordination environment (see ESI† Section S3).[14] We have termed the functionalized materials **SALI-*n*** (*i.e.* **SALI-1** through **SALI-28** where the CFG corresponding to the number is given in Scheme 1). The maximum incorporation of each CFG ligand was established by placing the functionalized **SALI-*n*** material into a fresh CFG solution for a second cycle of the reaction.

Each of the functionalized materials was examined by powder X-ray diffraction (PXRD) (Fig. 2c and ESI†). The PXRD patterns of all **SALI-*n*** materials showed no sign of degradation of the parent framework; slight differences in relative diffraction peak intensities were observed, due to changes in the electron density introduced by CFG ligands.[14] Thermogravimetric analysis (TGA) showed that the stability of the **SALI-*n*** materials depends on the identity of the corresponding CFG ligand (Section S6, ESI†).

The porosity of each **SALI-*n*** material was evaluated by recording 77 K N_2 adsorption isotherms. In each case, there was a reduction in gas uptake and the Brunauer–Emmet–Teller

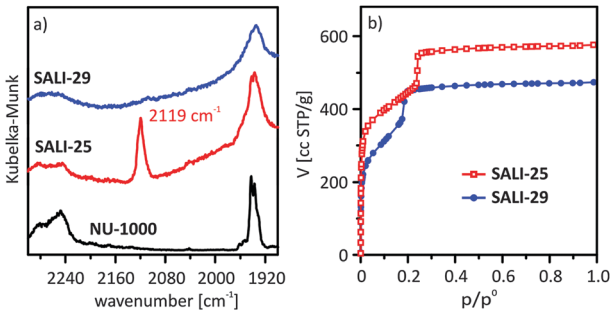

Fig. 3 (a) DRIFTS data for: the parent **NU-1000**, acetylene functionalized **SALI-25** and the "click" product **SALI-29** highlighting the SALI and secondary functionalization processes; (b) N_2 adsorption isotherms at 77 K for **SALI-25** and **SALI-29**.

(BET) surface area (values ranged from 600–1700 $m^2\ g^{-1}$) in comparison to that of the parent material (Table S1, ESI†). Slight shifts in the mesoporous step at approximately 0.22 P/P_0 to lower pressures in the adsorption isotherms were seen, indicating a decrease of the channel diameter upon CFG incorporation (Table S1 and Section S6, ESI†).

Further evidence regarding the availability of secondary functional groups in **SALI-*n*** is provided by diffuse reflectance infrared Fourier transform spectroscopy (DRIFTS) measurements. In **NU-1000**, as described before,[13a,14] a peak appears at 3674 cm^{-1} which has been assigned to the terminal –OH groups while a shoulder at 3671 cm^{-1} is consistent with the bridging μ_3-OH groups observed for **UiO-66**.[16] For **SALI-*n***, apart from the remaining bridging –OH ligands observed at 3671 cm^{-1} (see figures in S3, ESI†), signature peaks relevant to the secondary functional groups can be clearly discerned: for example, ethyne stretching in **SALI-25** appears at 2119 cm^{-1} and similarly characteristic peaks relevant to the incoming functional groups in **SALI-21**, **SALI-23** and **SALI-24** can be discerned at 3485/3382, 1710, and 2123 cm^{-1}, respectively (see figures in S3, ESI†).

To demonstrate the chemical accessibility and utility of the MOF-incorporated CFGs, various secondary functionalization reactions were performed. Summarized in Scheme 1b (ESI† Section S4) are three representative examples: an acetylide/azide "click" reaction (**SALI-25**), imine formation (**SALI-21**), and quaternization of the nitrogen base (**SALI-27**). These widely used, high-yield secondary functionalization reactions were aimed at: (a) incorporating new functionalities that are not compatible with a free carboxylate moiety, (b) facilitating introduction of various metal-Schiff base catalysts, and (c) demonstrating incorporation of tethered ionic species potentially relevant to separations, catalysis and/or sensing.

A copper(I) catalyzed "click" reaction of benzyl azide with **SALI-25** was carried out in the presence of sodium ascorbate in DMSO with 62% yield after 2 h as determined by ^{1}H NMR spectroscopy (ESI† Section S5A). DRIFTS data summarized in Fig. 3 highlight the disappearance of the ethynyl stretching peak at 2119 cm^{-1} after the "click" reaction. While the PXRD pattern of the "click" product, **SALI-29**, indicates retention of the framework structure (ESI† Section S4), an N_2 isotherm reveals lower surface area and pore volume upon such secondary functionalization (Fig. 3b). Likewise, the azide moiety in **SALI-24** was successfully "clicked" using phenylethyne (S5B, ESI†). Similarly, **SALI-21** converted to the imine derivative **SALI-31** with a quantitative yield (Scheme 1b; S4C, ESI†) as confirmed by ^{1}H NMR and DRIFTS data. While a quantitative quaternization reaction of the pyridine moiety in **SALI-27** was observed following methyl iodide (MeI) treatment, no methanol was detected in the ^{1}H and ^{13}C NMR spectra, thus indicating that the μ_3-OH functionality remains intact under these conditions.

In summary, we have shown that **NU-1000** can be used as a platform material in conjunction with the utility of SALI to efficiently incorporate various carboxylic acid-based alkyl and aromatic secondary functional groups. The wide range of CFGs that can be incorporated *via* SALI points to a battery of potential utilities in chemical separations, catalysis, and storage. Successful secondary functionalization (*e.g.* click reactions and imine formation) further enhances the scope of SALI methodology, and demonstrates the required stability of materials synthesized by SALI for consecutive chemical treatments.

OKF and JTH gratefully acknowledge support from the Global Climate and Energy Project (work related to materials for CO_2 capture) and the U.S. Department of Energy, Office of Science, the Basic Energy Sciences Program (grant DE-FG02-08ER15967; work related to materials for chemical separations). WB acknowledges support from the Foundation for Polish Science through the "Kolumb" Program. This material is based upon work supported by the National Science Foundation under CHE-1048773.

Notes and references

1 (*a*) O. M. Yaghi, M. O'Keefe, N. W. Ockwig, H. K. Chae, M. Eddaoudi and J. Kim, *Nature*, 2003, **423**, 705–714; (*b*) G. Férey, *Chem. Soc. Rev.*, 2008, **37**, 191–214; (*c*) S. Horike, S. Shimomura and S. Kitagawa, *Nat. Chem.*, 2009, **1**, 695–704.
2 O. K. Farha, I. Eryazici, N. C. Jeong, B. G. Hauser, C. E. Wilmer, A. A. Sarjeant, R. Q. Snurr, S. T. Nguyen, A. Ö. Yazaydın and J. T. Hupp, *J. Am. Chem. Soc.*, 2012, **134**, 15016–15021.
3 (*a*) O. K. Farha, A. Ö. Yazaydın, I. Eryazici, C. D. Malliakas, B. G. Hauser, M. G. Kanatzidis, S. T. Nguyen, R. Q. Snurr and J. T. Hupp, *Nat. Chem.*, 2010, **2**, 944–948; (*b*) H.-C. Zhou, J. R. Long and O. M. Yaghi, *Chem. Rev.*, 2012, **112**, 673–674.
4 (*a*) L. Ma, C. Abney and W. Lin, *Chem. Soc. Rev.*, 2009, **38**, 1248–1256; (*b*) J. Lee, O. K. Farha, J. Roberts, K. A. Scheidt, S. T. Nguyen and J. T. Hupp, *Chem. Soc. Rev.*, 2009, **38**, 1450–1459.
5 L. E. Kreno, K. Leong, O. K. Farha, M. Allendorf, R. P. Van Duyne and J. T. Hupp, *Chem. Rev.*, 2012, **112**, 1105–1125.
6 (*a*) C. A. Kent, D. Liu, L. Ma, J. M. Papanikolas, T. J. Meyer and W. Lin, *J. Am. Chem. Soc.*, 2011, **133**, 12940–12943; (*b*) S. Jin, H.-J. Son, O. K. Farha, G. P. Wiederrecht and J. T. Hupp, *J. Am. Chem. Soc.*, 2013, **135**, 955–958; (*c*) H.-J. Son, S. Jin, S. Patwardhan, S. J. Wezenberg, N. C. Jeong, M. So, C. E. Wilmer, A. A. Sarjeant, G. C. Schatz, R. Q. Snurr, O. K. Farha, G. P. Wiederrecht and J. T. Hupp, *J. Am. Chem. Soc.*, 2013, **135**, 862–869; (*d*) C. A. Kent, B. P. Mehl, L. Ma, J. M. Papanikolas, T. J. Meyer and W. Lin, *J. Am. Chem. Soc.*, 2010, **132**, 12767–12769.
7 S. M. Cohen, *Chem. Rev.*, 2012, **112**, 970–1000.
8 (*a*) S.-T. Zheng, X. Zhao, S. Lau, A. Fuhr, P. Feng and X. Bu, *J. Am. Chem. Soc.*, 2013, **135**, 10270–10273; (*b*) T. M. McDonald, D. M. D'Alessandro, R. Krishna and J. R. Long, *Chem. Sci.*, 2011, **2**, 2022–2028; (*c*) Y. K. Hwang, D.-Y. Hong, J.-S. Chang, S. H. Jhung, Y.-K. Seo, J. Kim, A. Vimont, M. Daturi, C. Serre and G. Férey, *Angew. Chem., Int. Ed.*, 2008, **47**, 4144–4148; (*d*) O. K. Farha, K. L. Mulfort and J. T. Hupp, *Inorg. Chem.*, 2008, **47**, 10223–10225; (*e*) J. S. Seo, D. Whang, H. Lee, S. I. Jun, J. Oh, Y. J. Jeon and K. Kim, *Nature*, 2000, **404**, 982–986.
9 Y. H. Kiang, G. B. Gardner, S. Lee, Z. Xu and E. B. Lobkovsky, *J. Am. Chem. Soc.*, 1999, **121**, 8204–8215.

10 (*a*) W. Bury, D. Fairen-Jimenez, M. B. Lalonde, R. Q. Snurr, O. K. Farha and J. T. Hupp, *Chem. Mater.*, 2013, **25**, 739–744; (*b*) O. Karagiaridi, M. B. Lalonde, W. Bury, A. A. Sarjeant, O. K. Farha and J. T. Hupp, *J. Am. Chem. Soc.*, 2012, **134**, 18790–18796; (*c*) T. Li, M. T. Kozlowski, E. A. Doud, M. N. Blakely and N. L. Rosi, *J. Am. Chem. Soc.*, 2013, **135**, 11688–11691; (*d*) M. Kim, J. F. Cahill, Y. Su, K. A. Prather and S. M. Cohen, *Chem. Sci.*, 2012, **3**, 126–130; (*e*) B. J. Burnett, P. M. Barron, C. Hu and W. Choe, *J. Am. Chem. Soc.*, 2011, **133**, 9984–9987.

11 J. H. Cavka, S. Jakobsen, U. Olsbye, N. Guillou, C. Lamberti, S. Bordiga and K. P. Lillerud, *J. Am. Chem. Soc.*, 2008, **130**, 13850–13851.

12 H. Wu, T. Yildirim and W. Zhou, *J. Phys. Chem. Lett.*, 2013, **4**, 925–930.

13 (*a*) J. E. Mondloch, W. Bury, D. Fairen-Jimenez, S. Kwon, E. J. DeMarco, M. H. Weston, A. A. Sarjeant, S. T. Nguyen, P. C. Stair, R. Q. Snurr, O. K. Farha and J. T. Hupp, *J. Am. Chem. Soc.*, 2013, **135**, 10294–10297; (*b*) W. Morris, B. Volosskiy, S. Demir, F. Gándara, P. L. McGrier, H. Furukawa, D. Cascio, J. F. Stoddart and O. M. Yaghi, *Inorg. Chem.*, 2012, **51**, 6443–6445; (*c*) D. Feng, Z.-Y. Gu, J.-R. Li, H.-L. Jiang, Z. Wei and H.-C. Zhou, *Angew. Chem., Int. Ed.*, 2012, **51**, 10307–10310; (*d*) Y. Chen, T. Hoang and S. Ma, *Inorg. Chem.*, 2012, **51**, 12600–12602.

14 P. Deria, J. E. Mondloch, E. Tylianakis, P. Ghosh, W. Bury, R. Q. Snurr, J. T. Hupp and O. K. Farha, *J. Am. Chem. Soc.*, 2013, **135**, 16801–16804.

15 Under studied reaction conditions for SALI process we typically observed incorporation of 2–4 CFG per node, where higher acidity and lower steric hindrance of the incoming ligand resulted in the higher degree of functionalization, and in some cases the SALI reaction completes within 1 h (Section S5, ESI†).

16 L. Valenzano, B. Civalleri, S. Chavan, S. Bordiga, M. H. Nilsen, S. Jakobsen, K. P. Lillerud and C. Lamberti, *Chem. Mater.*, 2011, **23**, 1700–1718.

